A new case-depth estimation technique for induction-hardened plates based on dynamic response studies using laser Doppler Vibrometer

ARTICLE *in* PROCEEDINGS OF THE INSTITUTION OF MECHANICAL ENGINEERS PART I JOURNAL OF SYSTEMS AND CONTROL ENGINEERING · SEPTEMBER 2014

Impact Factor: 0.78 · DOI: 10.1177/0959651814548302

4 AUTHORS, INCLUDING:

Bishakh Bhattacharya

Indian Institute of Technology Kanpur

64 PUBLICATIONS **157** CITATIONS

SEE PROFILE

A new case-depth estimation technique for induction-hardened plates based on dynamic response studies using laser Doppler vibrometer

Mohan K Misra, Bishakh Bhattacharya, Onkar Singh and A Chatterjee

Proceedings of the Institution of Mechanical Engineers, Part I: Journal of Systems and Control Engineering published online 5 September 2014
DOI: 10.1177/0959651814548302

The online version of this article can be found at:
http://pii.sagepub.com/content/early/2014/09/04/0959651814548302

Original Article

Institution of MECHANICAL ENGINEERS

Journal of SYSTEMS AND CONTROL ENGINEERING

Proc IMechE Part I:
J Systems and Control Engineering
1–14

DOI: 10.1177/0959651814548302
pii.sagepub.com
SAGE

A new case-depth estimation technique for induction-hardened plates based on dynamic response studies using laser Doppler vibrometer

Mohan K Misra[1], Bishakh Bhattacharya[2], Onkar Singh[3] and A Chatterjee[2]

Abstract

This article presents the effect of case depth due to surface hardening on the dynamic response of steel alloy–based circular plate. It indicates that such changes significantly affect the high-frequency response, especially, resonating modes and corresponding damping ratios of the plates. As the circular steel plates are quite rigid and hence the frequency responses are very small, a high precision three-dimensional laser Doppler vibrometer with a minimum velocity measurement capacity of 0.01 m/s is used to obtain the modal response. A statistical approach based on response surface methodology is then applied to obtain the correlation between the dynamic response of the system and the effective case depth. Also, another sensitive parameter termed as curvature change factor is introduced for the determination of the hardened layer thickness on the basis of laser Doppler vibrometer data. Thus, a new technique of condition monitoring of case-depth profile of steel plates based on non-contact dynamic response of the system has been established.

Keywords

Induction hardening, case-depth profile, dynamic response, three-dimensional laser Doppler vibrometer, curvature change factor, response surface methodology

Date received: 9 April 2014; accepted: 24 July 2014

Introduction

Surface/through hardening is most essential for improving wear resistance and strength of steel components. It is achieved when a selected surface or the entire object is subjected to a cycle of heating and quenching.[1] However, the hardening process requires careful monitoring of the system parameters to obtain a controlled case-depth profile which is generally carried out using induction hardening process.

Electromagnetic induction hardening is an energy-efficient, in-line, heat-treatment process widely used in automotive industry to surface-harden automotive parts at the lowest possible cost. The substitution of induction hardening for furnace hardening may lead to savings of up to 95% of the energy used in the heat-treating operations.[2] Also, such process causes significant weight-saving in automotive power-train components, further saving energy and manufacturing cost. Proper control of induction hardening process hinges on appropriate selection of coil design, selection of excitation frequency, and timing of heating and quenching. This process is generally based on trial and error which incurs loss of material and time. To minimize the effect of these errors on the quality of induction, hardened sample is perceived to be a difficult task due to enormous system complexity.

It is generally observed that induction hardening process enhances the strength and wear resistance of the surface layer of the components at the cost of

[1]PhD Scholar, U P Technical University, Lucknow, India
[2]Department of Mechanical Engineering, Indian Institute of Technology, Kanpur, India
[3]Department of Mechanical Engineering, Harcourt Butler Technological Institute, Kanpur, India

Corresponding authors:
Mohan K Misra, SMSS Lab, NL#102, I I T Kanpur- 208 016 India.
Email: emkay@iitk.ac.in
Bishakh Bhattacharya, Department of Mechanical Engineering, Indian Institute of Technology, Kanpur- 208 016, India
Email: bishakh@iitk.ac.in

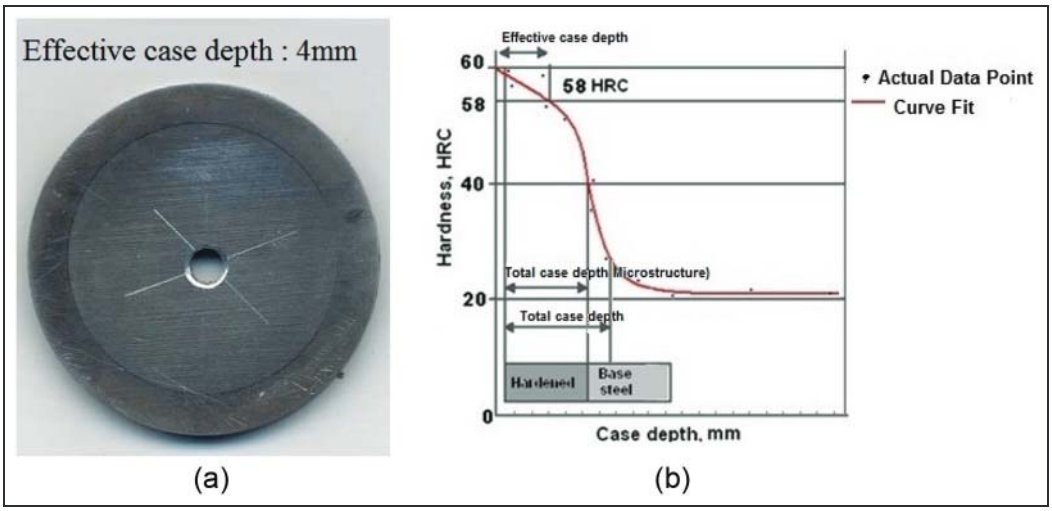

Figure 1. (a) EN-8 sample with ECD of 4 mm and (b) a typical profile of a surface-hardened EN-8 sample.

ductility and toughness.[2] Therefore, it is useful to estimate the mechanical properties of hardened samples based on the micro-structural condition at the subsurface region of a hardened component. As it is practically impossible to monitor the micro-structure directly, hence, it is imperative to devise a non-destructive evaluation (NDE) technique which can sense the change in system parameters due to finer micro-structure variations. The major advantage of using non-destructive techniques is to provide an economic way of achieving high-quality inspection which is not possible with the destructive testing methods used to determine the hardened layer profile of shafts and other components. The methods commonly employed for measuring such case depth are visual (with an acid etch), chemical, mechanical, and non-destructive techniques.[3]

In this article, a brief overview of various non-destructive techniques, generally used for the measurement of case-depth profile, is presented. Next section discusses the use of a new dynamic response–based technique for this purpose. Modal parameters along with curvature change factor (CCF) have been shown to be effective in this direction. Subsequently, based on the dynamic response, a predictive model for effective case depth (ECD) has been developed. The results are further validated with the help of destructive studies. These are carried out for selected plates with varied case depths. It has been shown to be effective in predicting the case-depth profile accurately. Finally, conclusions are drawn based on the study.

An overview of case-depth measurement techniques

Before discussing on NDEs of hardness and case depth, it is important to distinguish between ECD and total case depth of any hardened steel sample. ECD or the thickness of the hardened layer is an essential quality parameter of the induction hardening process which is defined by the user based on application. The darker periphery of a typical round plate, as shown in Figure 1(a), shows the ECD of a hardened sample.

For a typical round plate, ECD is determined as that region or distance from periphery where desired hardness value is measured. In our case, it is 58-60 HRC for components like spindle shaft. Figure 1(b) shows ECD as typically 65% of the total micro-structure case depth. Micro-structure case depth is considered to be 75% of the total case depth which is also defined as the distance from periphery where hardness value is 10% more than the hardness at the core of the steel sample.[4]

To ascertain hardness and case depth, NDE techniques are used based on elastic, electrical, and magnetic material properties. In the case of ferrous materials, often magneto elastic parameters are also used. These properties may vary, depending on micro-structure, macro-stresses, micro-stresses, anisotropy, and further intrinsic properties.[5,6]

A review of various NDE-based case-depth detection procedures brings out following major techniques that are commonly employed:

1. Use of the magnetic and magneto-electrical characteristics;[7]
2. Sound velocity of ultrasonic waves;[8,9]
3. Backscatter of ultrasonic waves;[10]
4. Other techniques, for example, potential drop measurement.[11]

These procedures are briefly described in the following:

1. In this technique, the magnetic Barkhausen emission (MBE) from the hardened profile of carbon steel is compared with non-hardened samples and the extent of surface hardening is predicted.[12] Generally, the hysteresis loop shows a distortion with a sudden reduction in the rate of

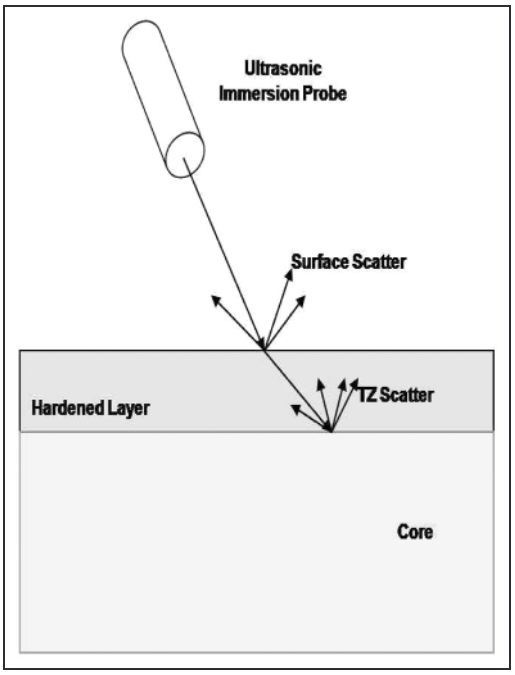

Figure 2. Scatter of ultrasonic waves from the surface and transient zone of an induction-hardened specimen.

magnetization (dB/dH) indicating the presence of a distinctive boundary of hardened surface. The systematic changes in the MBE profile for different voltages applied during induction heating indicate the dynamic changes in micro-structural configurations. However, this process is effective in measuring low case depth only. The limiting factor for MBE is the attenuation of the signal source by eddy currents as it propagates through the material, leading to a maximum measurement depth of about 1 mm,[5,13] depending on the excitation frequency, frequency range, and material properties. The domain wall motion that generates MBE also causes a release of elastic energy known as magneto-acoustic emission (MAE), which has a greater measurement depth, and hence offers a complementary technique to extend the measurement depth up to 8 mm for the characterization of surface treatments in steel.[12]

2. From Figure 1, it is evident that the change in micro-structure generates several interfaces in a hardened steel beam and thus causes sound waves to get reflected at the interfaces which form the basis of ultrasonic testing (UST). Theiner et al.[14] have performed ultrasonic tests, in which sound waves of high frequency (10–25 MHz) are transmitted into the steel sample (rod placed in a water tank). The transducers have sensed the boundary between soft core and hardened layer as discontinuities and therefore predicted the depth of hardened layer as a function of time delay or time-of-flight (TOF) between the front surface reflection and the reflection at the transition zone.[6,14] This procedure is further modified to develop ultrasonic-based backscattering technique.
3. In ultrasonic backscatter technique (USBT), the specimen and ultrasonic probe are both immersed in a tank filled with water (see Figure 2). The placement of probe is made in such a way that it can send shear waves into the specimen; it is inclined at an angle from the orthogonal cross-sectional plane of the specimen.[15] Ultrasonic backscattering phenomenon occurred twice, the first echo takes place at the surface of the specimen due to surface roughness and results in the return of part of the energy to the probe. Ultrasonic energy also enters the hardened layer as a shear wave. The hardened surface layer is made of fine martensite structure and thus, no scatter of ultrasonic wave takes place in this region. However, when the shear wave reaches the transient zone (TZ), where martensite structure is gradually converted to ferrite-pearlite structure which is of a larger grain size, once again, the energy is scattered at the grain boundaries. This transition zone backscatter forms the second echo, as shown in Figure 2.
4. In alternating current potential drop (ACPD) technique, the standard values of conductivity and permeability of an unhardened rod are used to calibrate the experimental results of induction-hardened steel rods.[11] The hardened rod is assumed to be made up of a homogeneous soft core which is surrounded by a case hardened layer of uniform thickness. The values of case depth are obtained by parameter fitting to minimize a penalty function using multi frequency potential drop measurements. This method has shown a reasonable agreement with hardness values found using Rockwell hardness measurements.

A comparison of different traditional NDE processes used for surface profile estimation has been shown in Table 1. Table 1 shows that ultrasonic and MBE-based techniques are highly accurate. However, these are very expensive and difficult to be carried out in real time.

The study of dynamic response of a system could provide very significant indications toward the change of micro-structure or phase change of a material.[16] The next section presents a brief description of the current uses of dynamic response in terms of damage detection of various mechanical components. Subsequently, this technique is extended for case-depth prediction.

Dynamic response for system identification

The use of dynamic response in structural health monitoring is getting popular nowadays. The changes in dynamic responses such as natural frequencies, modal damping, and mode shapes of the structures are

Table 1. Comparison of different traditional NDE processes.

Method	Phenomenon	Range of measurement	Accuracy (%)
MBE and MAE[12]	Electro-magnetism	7–8 mm	~1.5%
UST[14]	Reflection of sound wave	2 mm	Less than 5%
USBT[15]	Reflection of sound wave	2–4 mm	~0.5%
ACPD[11]	Change of conductivity and permeability	2 mm	20%–24%

MBE: magnetic Barkhausen emission; MAE: magneto-acoustic emission; UST: ultrasonic testing; USBT: ultrasonic backscatter technique; ACPD: alternating current potential drop.

observed when changes in physical properties of the structures occur due to damage. Therefore, through supervised training, this knowledge-base of dynamic response proves helpful for damage identification. Measuring changes in natural frequency to detect damage often face limitation, as these are mostly coupled with inherent noise, especially in large structures. Sometimes very small changes in natural frequency (which is registered as noise) attribute due to temperature difference and change of mass and hence may generate false results.[16] The location of damage in flat plate based on finite element analysis is discussed by Kumar et al.[17] They have shown significant changes in flexural vibration modes for flat plate while assuming modulus of elasticity in the damaged zone to be close to zero. Hanagud et al.[18] have noted the characteristics of lower-order curvature modes, which are found to be distinctive for healthy and damaged structures. Thereafter, a mathematical relationship for the dynamic parameter (difference in amplitude of curvature mode shapes) is employed to predict the loss of local stiffness which was caused as a result of damage. For small change in natural frequency, the frequency-based damage detection methods are ineffective in predicting the extent and location of damage. Luo and Hanagud[19] have suggested a detection algorithm which is based on integral change in curvature mode shape of a structural beam and is found to be a better index for damage detection.

Thus, the literature survey indicates that the dynamic response of a system in various forms, namely, displacement, velocity, natural frequency, damping, modal frequencies, and mode shapes, has been used extensively for damage detection. As surface hardening is expected to cause local changes (comparable to damages in structures) in the disk structure, hence, similar techniques could also be employed to detect the hardening profile. The following section provides a brief description of the changes in steel structure that occurs during surface hardening and how it can affect the mechanical property of the plate.

Dynamic response of hardened plate

Medved and Bryukhanov[20] have shown that in accordance with Born's theory, the reduction of Young's modulus is inevitable when distortion of the crystal lattice occurs in a crystalline system as a result of any hardening process. It is well known that medium carbon steel (C: 0.45%) while undergoing induction hardening process, at temperatures above 730 °C, transforms into austenite phase. As soon as the steel components slowly get cooled, the austenite phase changes into ferrite structure. The dynamic response of hardened steel plate is expected to respond to such phase transformation. In the current study, modal analysis of EN-8 samples is carried out using laser Doppler vibrometer (LDV), and the vibration signature as well as damping analysis are carried out for unhardened and hardened samples in order to obtain a correlation between thickness of the hardening layer and system response. Figure 3(a) and (b) shows typical frequency response, in pre and post hardening stage, explaining this concept very well.

It is evident that a part of excitation signals, generated from shaker, traveled through hardened surface where some part is reflected from interface between soft and hardened layers (reflected signal shown in red in Figure 3(b). Therefore, the resultant wave signal (made up of refracted as well as reflected wave) produces change in natural frequency ν_n and damping ratio ζ. This change in dynamic response will be different for varying case depths and thus may prove beneficial as an important indicator for predicting ECD.

It may be noted from Figure 4 that a hardened specimen shows significant change in the natural frequency in comparison to the unhardened sample. Applicability of experimental modal analysis for predicting in-process case depth is discussed elaborately in the following sections.

Brief description of the polytec scanning vibrometer (PSV) three-dimensional measurement method

In laser-based scanning, the scanner sends a low-power laser light on the surface of the vibrating object (see Figure 5), following a grid/mesh which has been given as an input to the system.

A charge-coupled device (CCD) camera integrated with the scanner records the position coordinates and light intensity at each point on the surface of the object. Taking recourse of the Doppler effect, these data are transformed to obtain the velocity response of every scanned point. The velocity response profile is then digitally integrated to obtain the deflection response.

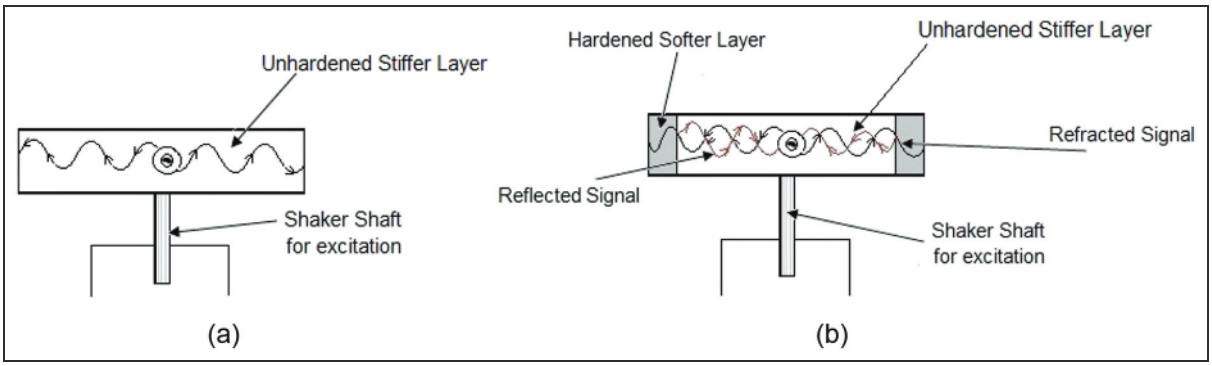

Figure 3. (a) Dynamic response of unhardened component and (b) dynamic response of hardened sample.

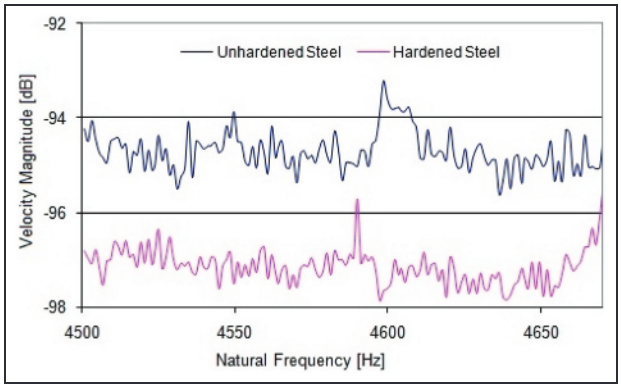

Figure 4. Change in dynamic response due to hardening of steel sample.

This procedure is carried out for all the predefined points on the surface of the object to get the complete operational deflection shape (ODS) of the object under dynamic loading. The three-dimensional (3D) LDV is a laser-based non-contact vibration measuring instrument which consists of three measuring scan heads capable of measuring the velocity and displacement along any three specified directions yielding full information of the 3D ODS. The minimum detectable vibration speed using this system is 0.01 m/s (at 1 Hz resolution), while the maximum speed is of 10 m/s. A function generator (NI-671x) contained in the system is used for generating excitation signals in the frequency range of 0–80 kHz. The LDV can measure vibrations up to 30 MHz range with very linear phase response and high accuracy. For the dynamic excitation of the EN-8 sample, an electro-dynamic shaker is used. A power amplifier (make: LDS, PA500L series) is connected to the shaker for the purpose of amplifying the excitation signal generated by the LDV system. During the experiment, a pseudo random signal in the frequency range of 0–7500 Hz is used for the excitation of the samples (Table 2).

Measurement of damping

A quantitative estimation of damping ratio ζ is obtained using the well-known half-power bandwidth method, as shown graphically in Figure 6. The damping ratio, ζ, can be determined using the following relationship

$$\zeta = \frac{\Delta\nu}{2\nu_p} \qquad (1)$$

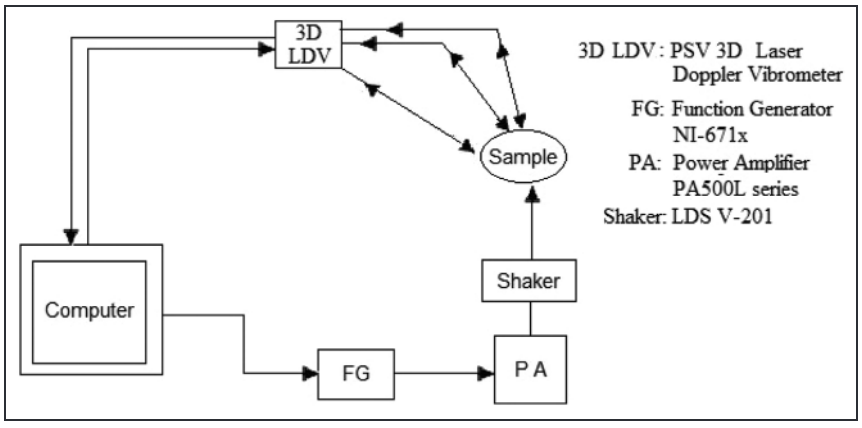

Figure 5. A schematic diagram of the experimental setup.
LDV: laser Doppler vibrometer.

Table 2. Details of the excitation signal used in 3D scan mode.

Excitation signal	Pseudo random
Frequency range	0–7500 Hz
FFT lines	1600
Window	Rectangle
Averages	10 (complex)
Velocity decoder	VD-09 digital decoder (velocity range: 0–10 mm/s)

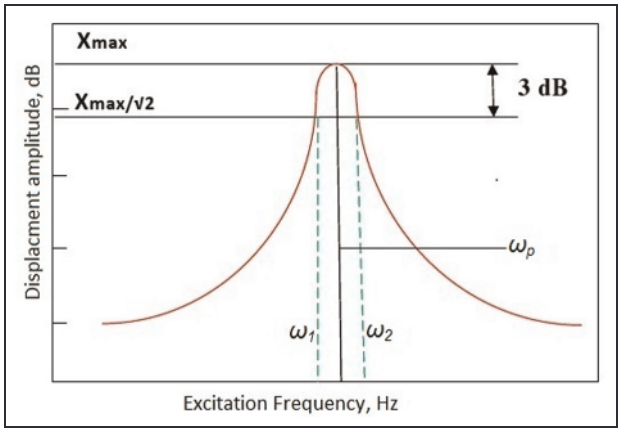

Figure 6. Measuring damping using 3-dB method.

$\Delta\nu$ is determined from the half-power points (ν_1 and ν_2), as shown in Figure 6.

The loss factor, η, can be obtained from strain energy density using the following relationship

$$\eta = \frac{\Delta U}{2\pi U_{max}} \quad (2a)$$

$$\eta \approx 2\zeta \quad (2b)$$

where U_{max} is the maximum strain energy stored in the system and ΔU is damping capacity for the sample disk.

Experimentation on dynamic response study

Sample preparation

EN-8 steel samples with diameter of 38 mm and thickness of 32 mm are hardened under varying process parameters on Inductotherm make 250 kW, 3–10 kHz induction heater model UP-12. Table 3 shows process parameters which produced samples with ECD of 4, 7, and 12 mm.

In order to achieve high-amplitude vibration response from experimental EN-8 samples using LDV, a very thin slice of 2.5–2.6 mm was cut with copper electrode in electrode discharge machine (EDM). The EDM was used to avoid apparent changes in case depth or hardness of the samples. Steel samples were then coated with developer so that the laser signals could easily get reflected from the surface to achieve accurate results. Experiments are carried out with an increased amplifier gain of 2.5, in order to have sufficient excitation of the high-frequency modes. Time required for the complete scan depends on the number of scan points defined and fast fourier transform (FFT) parameters. In the present analysis, only 25 scan points were defined due to smaller size of EN-8 sample (see Figure 7(c)). Figure 7(a)–(c) shows the overall test setup, the disk mounted on the shaker and scanning point representation, respectively.

Dynamic response results for case-depth prediction using response surface methodology

Response surface methodology (RSM) is a useful tool for predicting the behavior of response characteristics for any process especially manufacturing. It helps to analyze the effect of input parameters on output using different statistical and mathematical methods.

Following are the requisites to utilize RSM for predicting response characteristics of a process:

1. Data collection for those independent variables which influence the system greatly;
2. Prediction of suitable model of the system for results based on the experiments.

In this pursuit, Abou-El-Hossein et al.[21] predicted the cutting force in end-milling operation of tool steel, using the cutting force equations developed with the help of RSM. The effects of all the input parameters, for example, cutting speed, fed rate, radial depth, and axial depth of cut, were studied to develop predictive model for cutting force. Similar literatures are available, where RSM is successfully used for predictive modeling

Table 3. Process parameters to obtain output with desired ECD.

Number	Process parameter	Value to obtain 4-mm ECD	Value to obtain 7-mm ECD	Value to obtain 12-mm ECD
1	Frequency	10 kHz	2 kHz	2 kHz
2	Power	65 kW	65 kW	65 kW
3	Current	105 A at 415 V	105 A at 415 V	105 A at 415 V
4	Scanning speed	1300 mm/min	980 mm/min	550 mm/min
5	Quench flow	40 L/min at 22 lbf/in^2	40 L/min at 22 lbf/in^2	40 L/min at 22 lbf/in^2
6	Quench temperature	32 °C	32 °C	32 °C
7	Surface hardness	58–60 HRC	58–60 HRC	58–60 HRC

ECD: effective case depth.

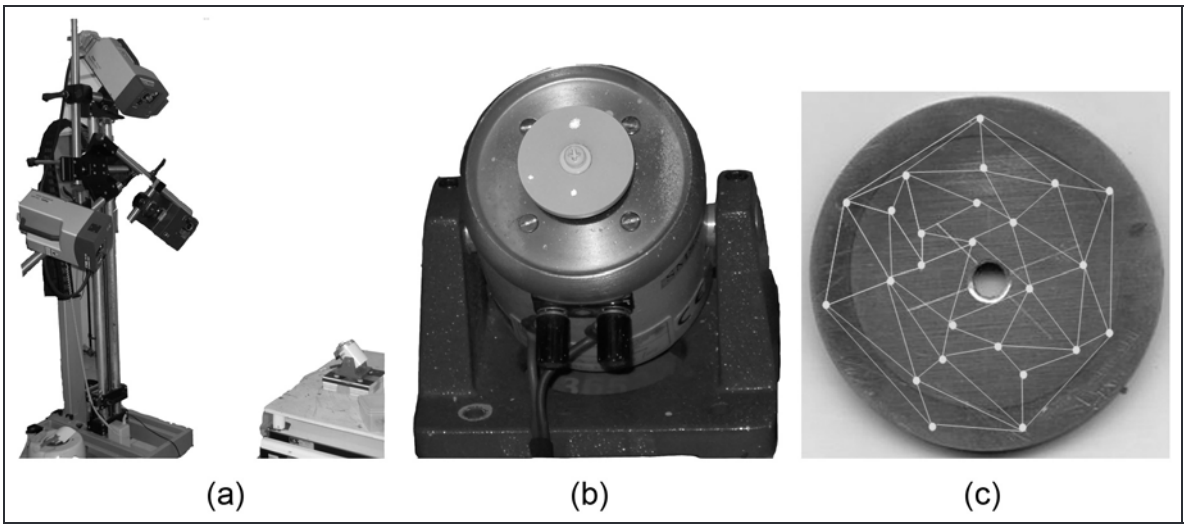

Figure 7. (a) PSV 3D experimental setup, (b) EN-8 sample mounted on electro-dynamic shaker, and (c) sample with scanning point representation.

of response characteristics of wide range of industrial processes.

Our approach is to first build a model based on known ECD samples and then validate this model through destructive testing. Therefore, the suggested model would be helpful for predicting the case-depth profile of output samples for which we only know the dynamic response. In our present study, 48 EN-8 hardened samples are taken. These hardened samples are essentially the output of induction hardening process based on parameters presented in Table 3. This is done to ensure a robust model for predicting ECD in concurrence with dynamic response parameters. With the help of LDV, output graph for velocity magnitude in decibels and frequency response of all the samples are obtained. Once analyzing the results, dynamic response parameters such as natural frequency, damping ratio, and loss factor are identified. These parameters are used as input variables for Design-Expert software for predicting the response factor which is case depth in our case. This is a statistical software package which uses design of experiment (DOE) methods for optimization of process. The design summary, presented in Table 4, is a brief description of input data and proposed analysis method provided to the software for case-depth predictive model using RSM. Here, design model refers to the choice of model order and nature of response. It is used for simulating the nature of the input–output relationship on the basis of supplied data to the software, which is the information gathered from 48 EN-8 samples. Since the variation in minimum and maximum values of damping ratio is very small, standard deviation value for damping ratio did not appear in this presented design summary.

Results and discussion

Table 7 presented in Appendix 1 shows the experimental results corresponding to 16 hardened samples with ECD of 4, 7, and 12 mm each, which are output of induction hardening process based on parameters mentioned in Table 3. Therefore, samples are classified based on their known ECD values. Response plots and animated mode shapes were studied after the scan to identify the nature of the modes and match between the similar modes of different samples.

Figure 8 shows the rigid body mode and first bending mode for an unhardened plate while subjected to base excitation. The natural frequency obtained, for the first bending mode, is 4691 Hz and the corresponding damping factor is 0.024.

The dynamic response of hardened plate with 12 mm case depth as shown in Figure 9 appeared shifted, and natural frequency corresponding to the first bending mode is obtained as 4568 Hz. A similar change in natural frequency of the first bending mode for hardened plate with 4 and 7 mm case depths has also been observed. A drop of 2%–2.5% in natural frequency is observed due to hardening of the steel plate.

This observation is indicative in terms of predicting the case depth obtained as a result of induction hardening procedure. In order to develop a predictive model for case depth using dynamic response results, data presented in Table 7 (see Appendix 1) are used as historical data under response surface environment with Design-Expert software.

Figures 10 and 11 show the scatter plot related to natural frequency and damping ratio, respectively, for samples with different case depths. It may be noted that while the damping ratio has not varied much from sample to sample, the natural frequency shows variation of about 0.5% from the mean value. This is possible due to variation of ECD during induction hardening process.

Figure 12 shows scatter plot between natural frequency and damping ratio. Also from this figure, it can be concluded that damping ratio increases with increase in case depth. This observation is supported well in

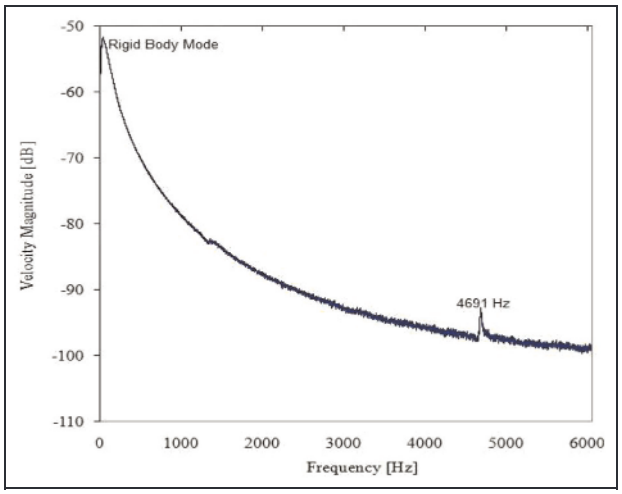

Figure 8. Natural frequency v_n obtained from unhardened sample.

findings of Visnapuu et al.[22] where it is discussed that heat treatment enhances inter-granular boundary stress level and thus improves damping. Possibly, this is the reason that with increase of case depth, damping ratio increases.

For the presented historical data, various combinations of process orders (i.e. Cubic, Quadratic, Mean, 2F1, linear, and so on) have been tested for obtaining the significance of process parameters and lack of fit. This significance test is needed to avoid any error or noise for the predicted output. Table 5 shows the analysis of variance (ANOVA), for concluding the best model for case-depth prediction. For linear process order, F value is found to be quite high. The high value of F suggests that there are very little chances ($\backslash$ 0.01%) of any error or noise. Therefore, reduced linear model for case-depth predictions proved as significant. Also, the absence of loss factor suggests the insignificance of loss factor parameter in the presented set of data for predicting the ECD.

Thus, ANOVA concluded the predicted model for case depth which is described in equation (3)

$$\text{Predicted ECD} = \square 55{:}718 + 0{:}0094\ 3\ v_n + 7512{:}77\ 3\ z \qquad \text{ð3Þ}$$

In order to establish the efficacy of this dynamic response–based innovative NDE technique, destructive testing of some of the experimental samples was carried out. Following section presents the validation of model for case-depth prediction as well as results obtained from micro-structure.

Validation of dynamic response technique

To establish the accuracy of results obtained from dynamic response–based predictive model, 6 samples out of 48 experimental samples were selected for further detailed testing. Micro-hardness and micro-structures provide definite information about the ECD of these experimental samples. Figure 13 shows the micro-structures of one of these samples which were obtained from metallurgical microscope model: RMM-2 using ProgRes CT3 camera.

The micro-structure is observed, at different places of the EN-8 sample, to ascertain the actual phases of steel. It is very clearly visible under the microscope at different resolutions (400 3 , 1000 3) that the middle layer of sample is having a mixture of ferrite and pearlite. The outer hard layer is pure martensite (needle-like structure).

The standard testing procedure for Rockwell hardness test method was adopted, and samples were investigated for average value of micro-hardness at different regions on those experimental samples (Figure 14). These regions are approximately 4 mm wide zone. It helps us to locate the steep drop of hardness value so that ECD can be identified. Table 6 shows the results which validate the case-depth prediction model very well.

CCF

While change in modal parameters may be directly linked to the system hardness, the determination of

Table 4. Design summary for RSM for case-depth predictive model.

Study type	Response surface						
Initial design	Historical data						
Design model	Quadratic						
Runs	48						
Factor	Units	Low actual	High actual	Mean	Standard division		
Natural frequency (v_n)	Hz	4558	4610	4582	15.808		
Damping ratio (z)		0.00217	0.00329	0.003	–		
Loss factor (h)		0.00434	0.0658	0.005	0.001		
Response	Units	Analysis	Minimum	Maximum	Mean	Standard division	Method
Case depth	mm	Polynomial	4	12	7.680	3.297	Reduced linear

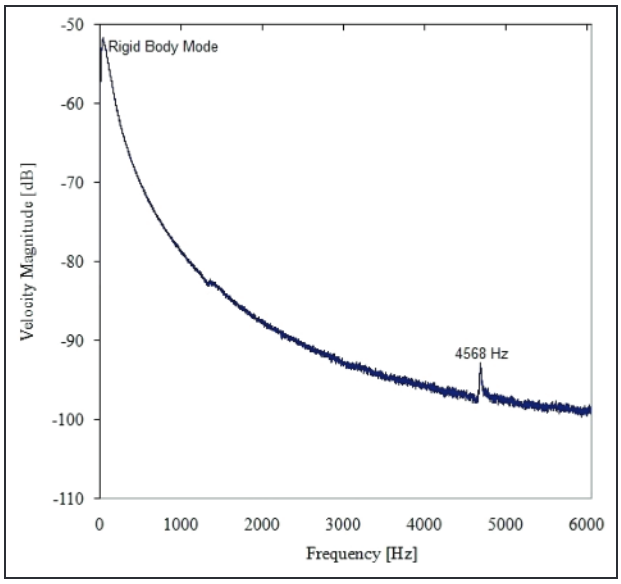

Figure 9. Natural frequency v_n obtained from hardened sample with 12 mm case depth.

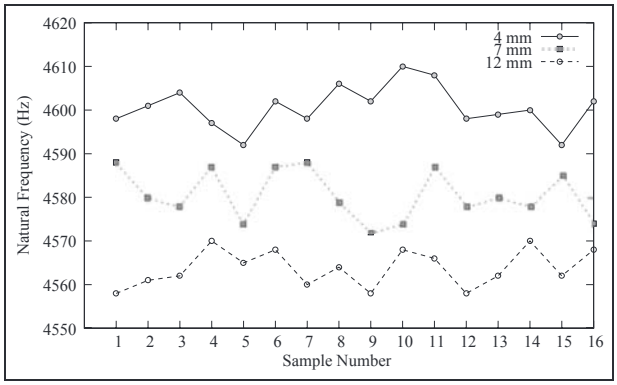

Figure 10. Natural frequency distribution across different case-depth samples.

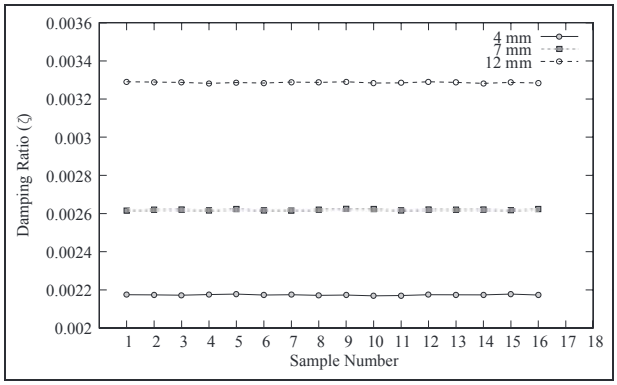

Figure 11. Damping ratio distribution across different case-depth samples.

hardness profile may need further analysis of the dynamic response. In case of health monitoring, damage detection algorithms are capable of extracting

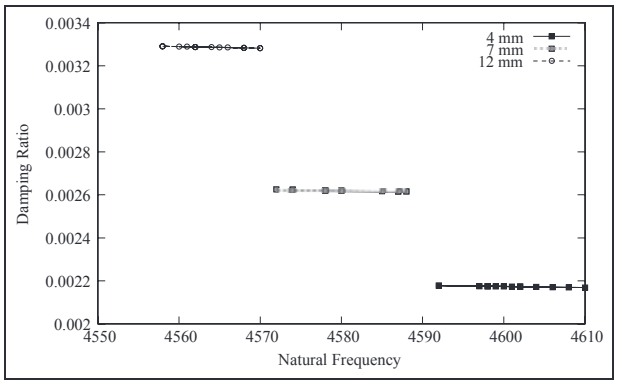

Figure 12. Damping ratio and natural frequency relationship across different case-depth samples.

useful information related to indication of damage location and magnitude. A similar index is developed here for obtaining the hardness profile by curvature change as an efficient parameter. The post-processing data obtained from LDV measurement give coordinates and velocity magnitude (m/s) for all the nodes (in our case there are 25 nodes) at v_n which is fundamental frequency corresponding to the bending mode. For every node, velocity, displacement, and mode shape are obtained from the LDV. The mode shape curvature (MSC) may be calculated from the measured displacement of mode shapes using a central difference approximation as

$$\phi''_{ji} = \frac{f_{(j+1)i} - 2f_{ji} + f_{(j-1)i}}{L^2} \qquad (4)$$

where ϕ'' is the mode shape corresponding to the transverse vibration, i is the mode shape number, j is the node number, and L is the distance between the nodes and represents spatial double differentiation.

Effect of hardening on EN-8 samples of various case depths can be more accurately predicted with the help of MSC. In case of induction hardening process, when a hardening layer is formed, the transverse stiffness is reduced while the magnitude of modal curvature increases. The absolute difference between the modal curvature of the unhardened and hardened samples is highest in the interface and reduces toward the core which is stiffer. The MSC criterion is defined here as the difference in absolute curvatures of the unhardened and hardened samples for each mode and represented as

$$MSC = D\phi''_i = \left| \phi''_{Unhardened\ j} - \phi''_{Hardened\ j} \right|_i \qquad (5)$$

The value of CCF is then calculated with the help of curvature values at the same nodes of unhardened and hardened steel samples considering all the mode shapes. Hence, it is the true comparison of dynamic response value if any change in micro-structure occurs in steel sample due to induction hardening process. In other words, change in case depth would lead to change in

Table 5. ANOVA for response surface reduced linear model.

Source	Sum of squares	df	Mean square	F value	p-value (probability . F)
Model	521.66	2	260.83	54589.34	\ 0.0001
A-natural frequency	0.12	1	0.12	25.36	\ 0.0001
B-damping ratio	64.52	1	64.52	13503.37	\ 0.0001
Residual	0.22	45	0.00478		
Lack of fit	0.20	27	0.00743	9.20	\ 0.0001
Pure error	0.015	18	0.00081		
Correct Total Sum of Squares	1462.49	75			

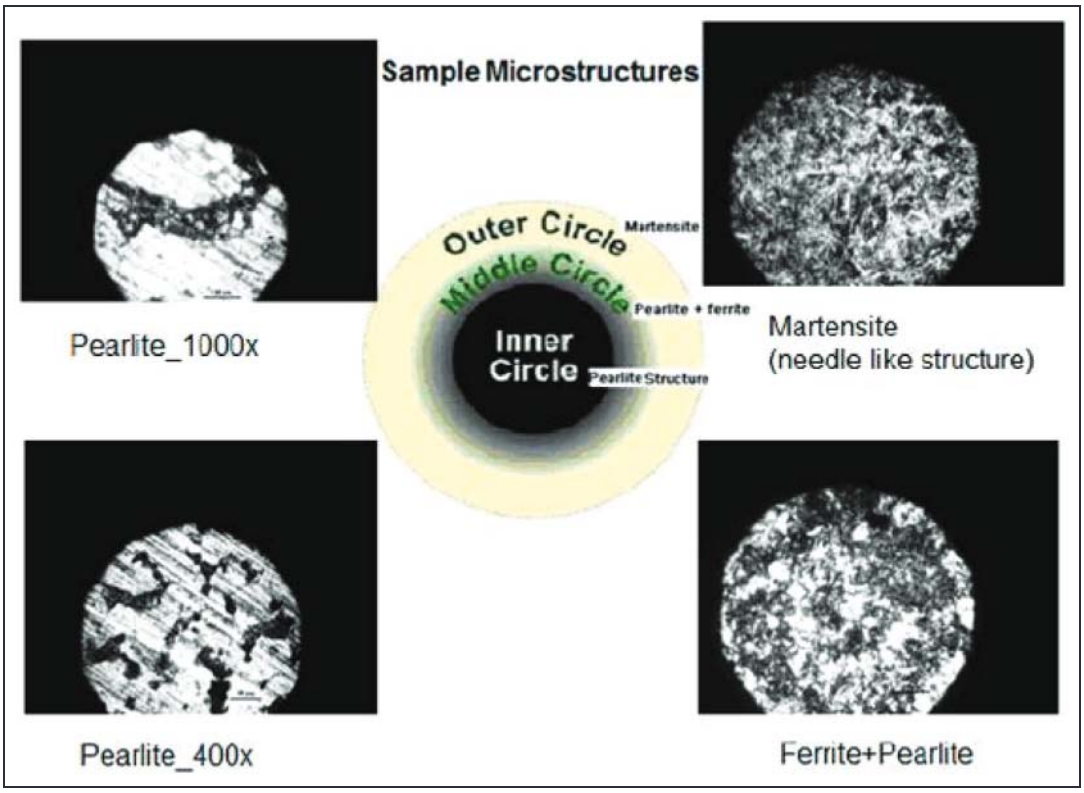

Figure 13. Micro-structure of unhardened and hardened layers of sample.

natural frequency as well as damping ratio; therefore, there will be a definite change in MSC and CCF as well. However, since all modes may not be equally sensitive to the hardness profile, the average change over a fixed number of modes gives the CCF defined in equation (6), which is more reliable to predict the effect of hardening. Thus

$$CCF = \frac{1}{N}\sum_{i=1}^{N}\left(\text{€}_{\text{Unhardened}_j} - \text{€}_{\text{Hardened}_j}\right)_i \qquad (6)$$

where N is total number of modes, i is the mode shape number, and j is the node number. Since in the current study, only one bending mode is observed in the frequency range of 7500 Hz, therefore, the value of MSC and CCF remains identical. This developed index called CCF is very useful in comparison to conventional micro-hardness methods. It is also useful for curved surfaces.

For calculating CCF, experimental process can be summarized as per flow chart presented in Figure 15. As per ASTM designation E18-12 (standard test method for Rockwell hardness testing for metallic materials), the indentation spacing defined to be 3d between two indents while 2.5d spacing from the edge, where d is the diameter of the indenter (Figure 16).

For the curved surface, it is highly likely to predict the case-depth profile with lesser accuracy, especially in zones where measuring hardness is not possible due to this minimum spacing constraint. On the other hand, no such restriction is applicable for CCF which is more continuous and can show a regular contour of hardened surface of test sample. This distinction clearly establishes the usefulness of this newly developed CCF index.

Table 6. Results for validation of predicted model.

Sample number	Harness at region A	Hardness at region B	Hardness at region C	Hardness at region D	Actual ECD	Predicted ECD	Absolute error
10	59	47	35	24	4	4.01	0.22%
16	60	45	32	22	4	3.96	2.42%
24	60	58	40	28	7	7.02	0.28%
30	58	59	36	26	7	7.01	0.14%
39	58	60	60	32	12	11.86	1.17%
43	60	60	59	30	12	11.88	1.00%

ECD: effective case depth.

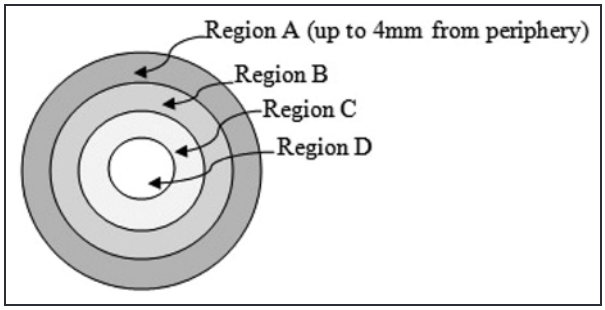

Figure 14. A schematic diagram of the experimental setup.

Figure 17 shows the CCF plot for a 4-mm case-depth hardened sample.

The green points correspond to the scanned nodes that lie inside the less stiff yet hardened layer (Figure 7(c)). The value of CCF is comparatively higher in this region. As we progress toward the core of the sample, the blue points appeared which is relatively stiff and non-hardened. Correspondingly, we see lower values of CCF in this region. Based on the study of a group of samples, a threshold value of approximately 8000 is fixed, which corresponds very well to the beginning of the unhardened layer.

Conclusion

In this article, a new dynamic response–based technique for the determination of induction hardening profile of steel samples is presented. To carry out this study, steel disks with three different hardness depths of 4, 7, and 12 mm were prepared. Metallurgical microscope images of the hardened and polished disks confirmed the presence of a two-layered profile. The outer hardened layer was martensite, which was followed by a ring of ferrite and pearlite below the hardened layer. The hardening layer was subsequently confirmed from the microhardness testing. Next, the disks were installed on a shaker in a cantilever mode, and the dynamic response of the top surface was obtained using LDV. By analyzing the response data, a noted difference between the unhardened and hardened sample was observed corresponding to natural frequency, damping ratio, and modal loss factor. With the help of available dynamic response data for 48 EN-8 samples, a case-depth predictive model was developed using RSM technique with the help of Design-Expert software. To further integrate the system parameters, a new metric named CCF is proposed which has been shown to have a strong correlation with the hardening profile.

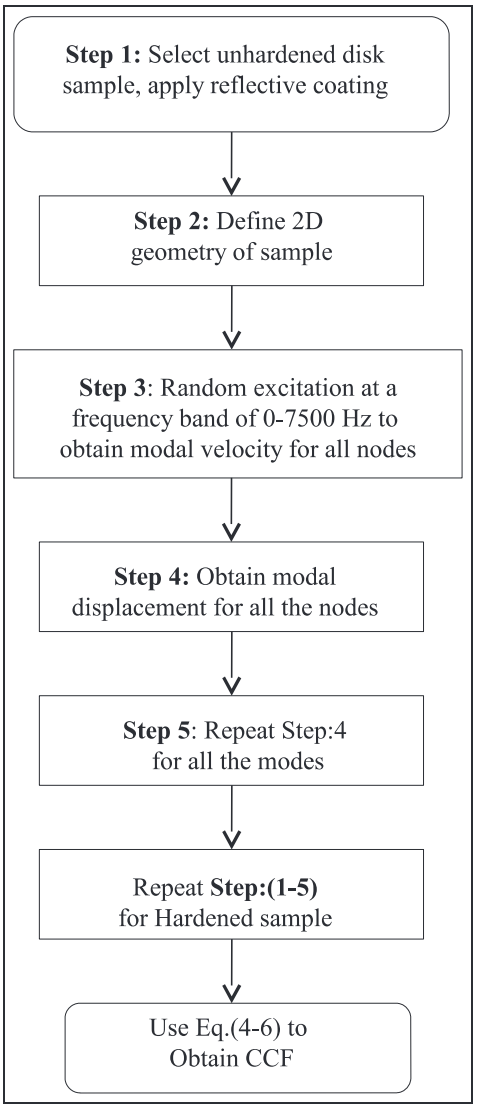

Figure 15. Flow chart for calculating CCF for steel samples.
2D: two-dimensional; CCF: curvature change factor.

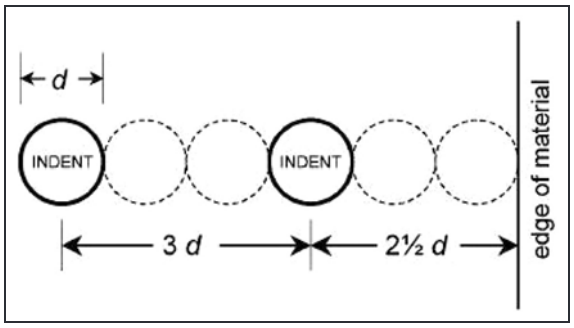

Figure 16. Schematic of minimum indentation spacing as per ASTM designation E18-12.

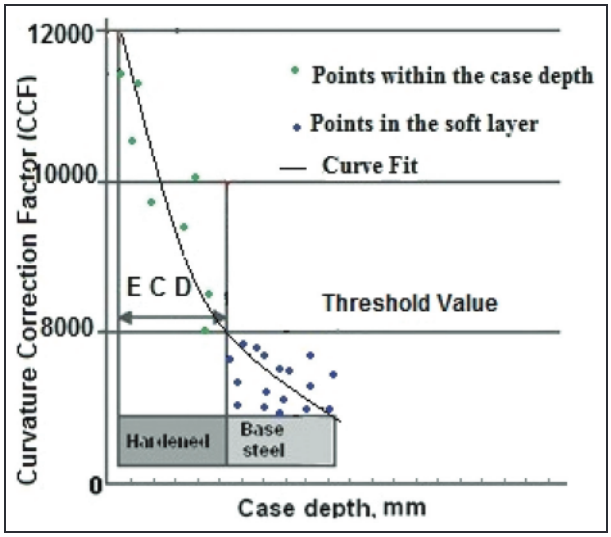

Figure 17. CCF for all 25 scanning points to predict ECD for hardened sample.
ECD: effective case depth.

In future, the CCF will be augmented with the other dynamic response parameters to obtain a better prediction of ECD. Also, this dynamic response–based expert system will be directly integrated to a control system for the effective control of induction hardening process for components of straight as well as curved surface profile.

Acknowledgements

The authors gratefully acknowledge partial support of UKIERI (Project: UKIERI/MDES/20120045) for disseminating the results in a national conference.

Declaration of conflicting interests

The authors declare that there is no conflict of interest.

Funding

This research received no specific grant from any funding agency in the public, commercial, or not-for-profit sectors.

References

1. ASTM A941-10a. Standard terminology relating to steel, stainless steel, related alloys, and ferroalloys. ASTM International, www.astm.org
2. Surface hardening of steels: Understanding the basics, 2002. OH: ASM International.
3. SAE J423:1998. Methods of measuring case depth. SAE International, 1998, www.sae.org
4. Czerwinski F. Thermochemical treatment of metals. In: Czerwinski F (ed.) Heat treatment: conventional and novel applications. 2012, pp. 73–112. Morn Hill, UK: InTech.
5. Moorthy V, Shaw B and Hopkins P. Surface and subsurface stress evaluation in case-carburized steel using high and low frequency magnetic Barkhausen emission measurements. J Magn Magn Mater 2006; 299(2): 362–375.
6. Honarvar F and Zeighami M. Application of signal processing techniques to case depth measurements by ultrasonic method. In: Proceedings of the 17th World conference on nondestructive testing, Shanghai, China, 25–28 October 2008, pp. 25–28.
7. Morgner W and Michel F. Some new results in the field of non-destructive case depth measuring. In: 9th European conference on non-destructive testing (ECNDT 2006), Berlin, 25–29 September 2006. The Open Access NDT Database.
8. Fuquen R, Leeper DR and Singh S. Process for measuring the case depth of case-carburized steel. US Patent 5,648,611, 1997.
9. Honarvar F, Sheikhzadeh H, Moles M, et al. Improving the time-resolution and signal-to-noise ratio of ultrasonic NDE signals. Ultrasonics 2004; 41(9): 755–763.
10. Baqeri R, Honarvar F and Mehdizad R. Case depth profile measurement of hardened components using ultrasonic backscattering method. In: 18th World conference on nondestructive testing, Durban, South Africa, 16–20 April 2012, pp. 1–8. Durban, SA: South African Institute for Non-Destructive Testing(SAINT).
11. Bowler JR, Huang Y, Sun H, et al. Alternating current potential-drop measurement of the depth of case hardening in steel rods. Meas Sci Technol 2008; 19(7): 075204.
12. Wilson JW, Tian GY, Moorthy V, et al. Magneto-acoustic emission and magnetic Barkhausen emission for case depth measurement in En36 gear steel. IEEE T Magn 2009; 45(1): 177–183.
13. Moorthy V, Shaw B and Evans J. Evaluation of tempering induced changes in the hardness profile of case-carburized EN36 steel using magnetic Barkhausen noise analysis. NDT&E Int 2003; 36(1): 43–49.
14. Theiner W, Kern R and Stroh M. Process integrated nondestructive testing of ground and case depth hardened parts. In: European conference on non-destructive testing (ECNDT 2002), Barcelona, 17–21 June 2002.
15. Good MS, Schuster GJ and Skorpik JR. Ultrasonic material hardness depth measurement. US Patent 5,646,351, 1997.
16. Chandrashekhar M and Ganguli R. Damage assessment of structures with uncertainty by using mode-shape curvatures and fuzzy logic. J Sound Vib 2009; 326(3): 939–957.
17. Kumar A, Fleming PJ and Bhattacharya B. Vibration suppression and damage detection in smart composite laminate using high precision finite element. In: SPIE smart structures and materials: nondestructive evaluation

and health monitoring, vol. 7982, San Diego, CA, 6 March 2011, pp. 1–16. Bellingham, WA: SPIE.
18. Hanagud S, Luo H and Lestari W. Detection of an edge notch defect by using a single mode based methods. In: 43rd Structures, structural dynamics and materials conference, Denver, CO, 22–25 April 2002, vol. 2, pp. 989–998. Reston, VA: American Institute of Aeronautics and Astronautics (AIAA).
19. Luo H and Hanagud S. An integral equation for changes in the structural dynamics characteristics of damaged structures. Int J Solids Struct 1997; 34(35):4557–4579.
20. Medved, AI and Bryukhanov, AE. The variation of Young's modulus and the hardness with tempering of some quenched chromium steels. Met Sci Heat Treat 1969; 11(9):706–708.
21. Abou-El-Hossein K, Kadirgama K, Hamdi M, et al. Prediction of cutting force in end-milling operation of modified AISI P20 tool steel. J Mater Process Tech 2007; 182(1):241–247.
22. Visnapuu A, Nash RW and Turner P. Damping properties of selected steels and cast irons. PA: US Department of the Interior, Bureau of Mines, 1987.

Appendix 1

Table 7. Experimental results for hardened steel samples. .

Sample number	Natural frequency (v_n)	Damping ratio (z)	Loss factor (h)	ECD (mm)	Sample number	Natural frequency (v_n)	Damping ratio (z)	Loss factor (h)	ECD (mm)
1	4598	2.175E2 03	4.350E2 03	4	25	4572	2.625E2 03	5.249E2 03	7
2	4601	2.173E2 03	4.347E2 03	4	26	4574	2.624E2 03	5.247E2 03	7
3	4604	2.172E2 03	4.344E2 03	4	27	4587	2.616E2 03	5.232E2 03	7
4	4597	2.175E2 03	4.351E2 03	4	28	4578	2.621E2 03	5.242E2 03	7
5	4592	2.178E2 03	4.355E2 03	4	29	4580	2.620E2 03	5.240E2 03	7
6	4602	2.173E2 03	4.346E2 03	4	30	4578	2.621E2 03	5.242E2 03	7
7	4598	2.175E2 03	4.350E2 03	4	31	4585	2.617E2 03	5.234E2 03	7
8	4606	2.171E2 03	4.342E2 03	4	32	4574	2.624E2 03	5.247E2 03	7
9	4602	2.173E2 03	4.346E2 03	4	33	4558	3.291E2 03	6.582E2 03	12
10	4610	2.169E2 03	4.338E2 03	4	34	4561	3.289E2 03	6.577E2 03	12
11	4608	2.170E2 03	4.340E2 03	4	35	4562	3.288E2 03	6.576E2 03	12
12	4598	2.175E2 03	4.350E2 03	4	36	4570	3.282E2 03	6.565E2 03	12
13	4599	2.174E2 03	4.349E2 03	4	37	4565	3.286E2 03	6.572E2 03	12
14	4600	2.174E2 03	4.348E2 03	4	38	4568	3.284E2 03	6.567E2 03	12
15	4592	2.178E2 03	4.355E2 03	4	39	4560	3.289E2 03	6.579E2 03	12
16	4602	2.173E2 03	4.346E2 03	4	40	4564	3.287E2 03	6.573E2 03	12
17	4588	2.616E2 03	5.231E2 03	7	41	4558	3.291E2 03	6.582E2 03	12
18	4580	2.620E2 03	5.240E2 03	7	42	4568	3.284E2 03	6.567E2 03	12
19	4578	2.621E2 03	5.242E2 03	7	43	4566	3.285E2 03	6.570E2 03	12
20	4587	2.616E2 03	5.232E2 03	7	44	4558	3.291E2 03	6.582E2 03	12
21	4574	2.623E2 03	5.247E2 03	7	45	4562	3.288E2 03	6.576E2 03	12
22	4587	2.616E2 03	5.232E2 03	7	46	4570	3.282E2 03	6.565E2 03	12
23	4588	2.616E2 03	5.231E2 03	7	47	4562	3.288E2 03	6.576E2 03	12
24	4579	2.621E2 03	5.241E2 03	7	48	4568	3.284E2 03	6.567E2 03	12